PCCP

PAPER

View Article Online
View Journal | View Issue

Cite this: *Phys. Chem. Chem. Phys.*, 2016, **18**, 3197

Temperature dependent radiative and non-radiative recombination dynamics in CdSe–CdTe and CdTe–CdSe type II hetero nanoplatelets

Riccardo Scott,†[a] Sebastian Kickhöfel,[a] Oliver Schoeps,[a] Artsiom Antanovich,[b] Anatol Prudnikau,[b] Andrey Chuvilin,[cd] Ulrike Woggon,[a] Mikhail Artemyev[b] and Alexander W. Achtstein†‡*[a]

Received 30th October 2015,
Accepted 21st December 2015

DOI: 10.1039/c5cp06623a

www.rsc.org/pccp

We investigate the temperature-dependent decay kinetics of type II CdSe–CdTe and CdTe–CdSe core–lateral shell nanoplatelets. From a kinetic analysis of the photoluminescence (PL) decay and a measurement of the temperature dependent quantum yield we deduce the temperature dependence of the non-radiative and radiative lifetimes of hetero nanoplates. In line with the predictions of the giant oscillator strength effect in 2D we observe a strong increase of the radiative lifetime with temperature. This is attributed to an increase of the homogeneous transition linewidth with temperature. Comparing core only and hetero platelets we observe a significant prolongation of the radiative lifetime in type II platelets by two orders in magnitude while the quantum yield is barely affected. In a careful analysis of the PL decay transients we compare different recombination models, including electron hole pairs and exciton decay, being relevant for the applicability of those structures in photonic applications like solar cells or lasers. We conclude that the observed biexponential PL decay behavior in hetero platelets is predominately due to spatially indirect excitons being present at the hetero junction and not ionized e–h pair recombination.

1 Introduction

Optically active semiconductor nanocrystals are a field of high current interest, since they have several unique electronic and optical properties, which can be engineered by size, composition, shape and surface modification.[1,2] In the last few years, a new class of colloidal 2D systems, the CdSe nanoplatelets, have been synthesized and studied.[3–10] They are characterized as nanosheets with a $n + 1/2$ monolayer (ML) thickness (as they are both sidedly Cd terminated[8,11,12]) and have atomically flat surfaces. (To avoid confusion: some authors use the number of Cd Layers instead of the $n + 1/2$ ML nomenclature, *e.g.* 5 ML for a 4.5 ML platelet.) Beyond the possibilities to alter physical properties by the above mentioned approaches, hetero nanoparticles offer a further possibility to tune their properties by engineering their in-built type I or II transition.[13–15]

The properties of CdTe–CdSe hetero nanodots and -rods have been investigated in systems of axial or spherical symmetry in the last few years.[16–22] Recent studies on the synthesis of type II CdSe–CdTe and CdTe–CdSe core–lateral shell nanoplatelets have investigated their morphology, the type II band offsets as well as the prolongation of the PL decay time with respect to core only nanoplatelets at room temperature.[23–25] In this report we concentrate on the temperature dependent photoluminescence (PL) decay dynamics and show that the observed luminescence decay is related to spatially indirect excitons, having a significantly prolonged lifetime with respect to core only nanoplates. We further concentrate on the yet open question whether carriers at the type II junction are present as spatially indirect excitons or separated electron hole pairs. Further we derive for the first time the temperature dependent radiative and non-radiative lifetimes from an analysis of the temperature dependent PL decay and quantum yield. The presented results strongly affect the applicability of hetero nanoplatelets in photonic applications like lasing media or charge extraction in hetero nanoparticle solar cells.

[a] *Institute of Optics and Atomic Physics, Technical University of Berlin, Strasse des 17. Juni 135, 10623 Berlin, Germany. E-mail: alexander.achtstein@tu-berlin.de*
[b] *Institute of Physico Chemical Problems, Belarussian State University, Leningradskaya str. 14, 220030 Minsk, Belarus*
[c] *CIC nanoGUNE Consolider, Tolosa Hiribidea 76, 20018 Donostia – San Sebastian, Spain*
[d] *Ikerbasque, Basque Foundation for Science, Maria Diaz de Haro 3, 48013 Bilbao, Spain*
† These authors contributed equally to this work.
‡ Present address: Department of Chemical Engineering, Optical Materials Section, Delft University of Technology, 2628 BL, Delft, The Netherlands.

2 Results and discussion

4.5 monolayer (ML) CdSe core only, 4.5 ML CdSe–CdTe nanoplatelets and inverse type II CdTe–CdSe nanoplatelets were synthesized according to recent literature.[23] Fig. 1 shows the absorption, PL and photoluminescence-excitation (PLE) spectra of 4.5 ML CdSe core only (a) and CdSe–CdTe core lateral shell platelets (b) as well as their transmission electron microscopy (TEM) characterization (insets (c)–(e)). Fig. 2 displays the corresponding data for the 3.5 ML CdTe only and the inverse CdTe–CdSe samples. The actual thickness of the CdSe and CdTe plates and lateral wings is n + 1/2 times the thickness of one monolayer[8,11,12] (zinc blende: d_{ML}^{CdSe} = 0.304 nm, d_{ML}^{CdTe} = 0.324 nm). Fig. 1(a) shows the characteristic 4.5 ML heavy hole (hh) exciton luminescence (orange) around 512 nm, whereas the PL peak of the hetero system is red shifted to 680 nm (b). From the corresponding absorption and PL spectra the hh absorption peaks of both the CdSe core at 512 nm and the CdTe shell at 555 nm can be identified. The PLE spectrum recorded at a type II transition wavelength of 680 nm clearly proves the formation of a CdSe–CdTe hetero junction, as the PLE spectrum resembles the cumulative absorption spectrum of the CdSe–CdTe nanoplatelets, in line with previous investigations.[23–25] The samples were embedded in a poly(lauryl acrylate) host matrix on quartz substrates for low temperature measurements.

Fig. 2 contains the same information for 3.5 ML CdTe core and CdTe–CdSe hetero nanoplatelets. Due to the stronger transversal confinement (thinner platelets) the corresponding CdTe hh and CdSe hh transitions are blue shifted with respect to Fig. 1. Fig. 3 shows that the 4.5 ML CdSe core only platelets are characterized by relatively fast PL decay times due to the giant oscillator strength effect (GOST) in 2D.[4,5] The PL decay itself is bi-exponential,[26] as can be seen by selected biexponential fits in Fig. 3(a). The convolution with the instrument response IRF (green curve) is taken into account. This biexponential decay is related to a dark-bright splitting of the lowest exciton state.[26] As shown in Fig. 3(b) the PL decay components of the CdSe core only nanoplatelets are fast and of the order of 200 ps for the short and 1–2 ns for the long component. However, this finding is only a prerequisite to compare with hetero nanoplatelets, on which this report is focused. In contrast to this fast recombination of core only CdSe nanoplatelets our 4.5 ML CdSe–CdTe

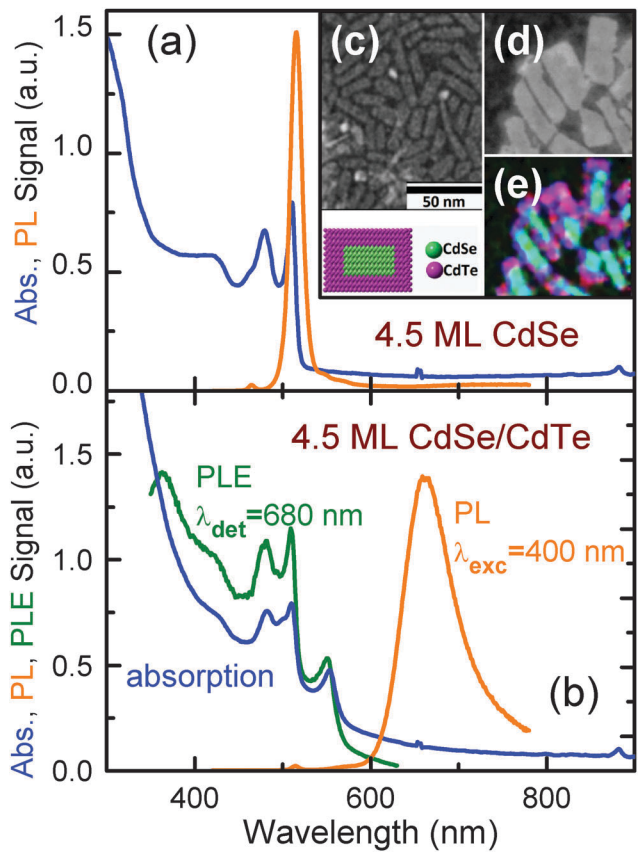

Fig. 1 Room temperature absorption, PL and PLE spectra of 4.5 ML CdSe core only (a) and 4.5 ML CdSe–CdTe hetero nanoplatelets (b). The PLE spectrum is recorded at the hetero platelet emission maximum at 680 nm. Inset: HAADF STEM images of the 16 × 8 nm^2 CdSe core (c), and 27 × 47 nm^2 CdSe–CdTe hetero nanoplatelets (d) as well as a color coded STEM-EDX elemental map (Te red, Se green and Cd blue) resolving the CdSe core (aquamarine) and CdTe lateral shell (pink) (e).

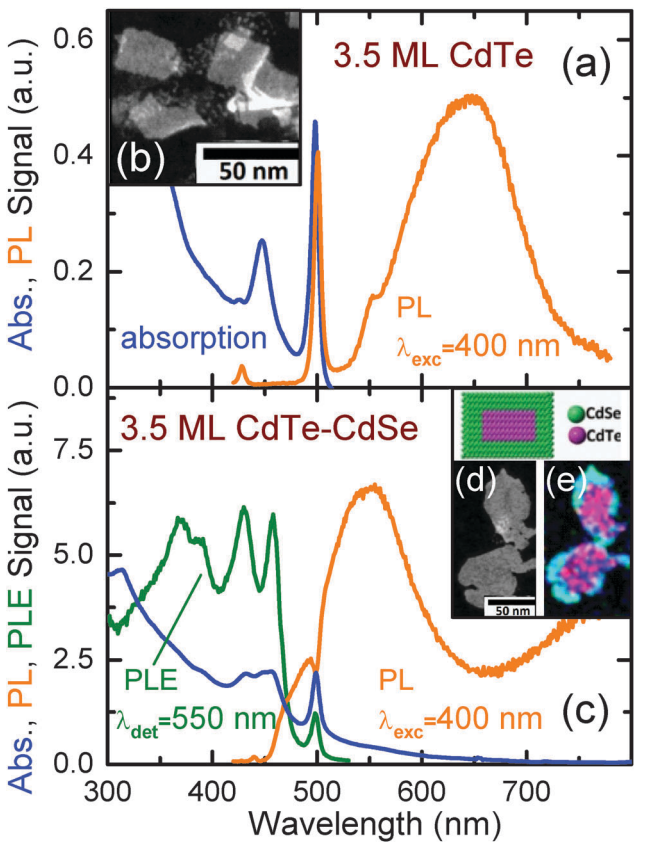

Fig. 2 Room temperature absorption, PL and PLE spectra of 3.5 ML CdTe core only CdSe platelets (a) with lateral size 42 × 35 nm^2 and 3.5 ML CdTe–CdSe hetero platelets with total lateral size of 70 × 58 nm^2 (c) having the same core size as in (a). Inset (b) shows a TEM image of the CdTe core platelets, whereas insets (d) and (e) show a color coded STEM-EDX elemental map of CdTe and CdSe in the heteroplatelets. The PLE spectrum in (c) is recorded at the hetero platelet emission maximum at 550 nm.

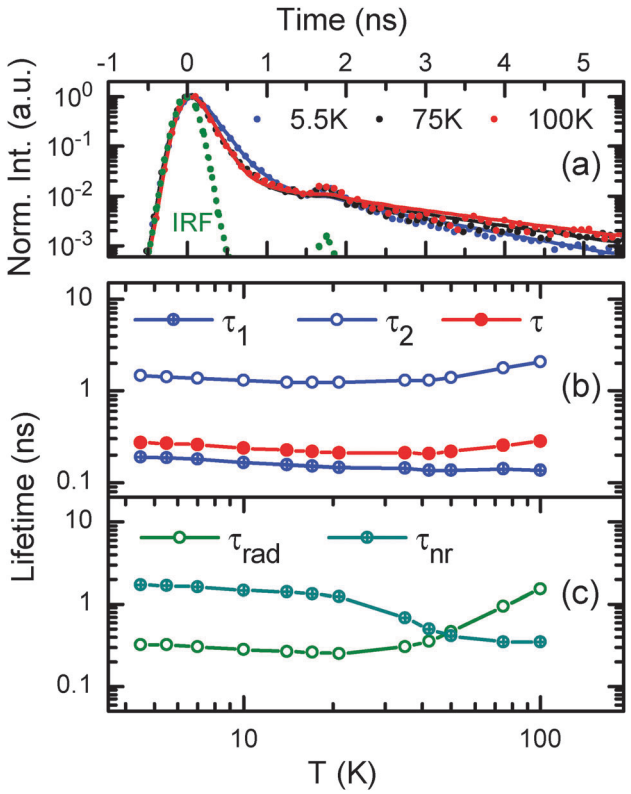

Fig. 3 (a) Normalized time resolved photoluminescence of 4.5 ML CdSe core only platelets recorded at the spectral maximum of the emission for selected temperatures (5.5, 75 and 100 K). The biexp. fits (solid curves) take the convolution with the instrument response function (IRF, green curve) into account. The IRF is recorded at the emission wavelength of the excitation laser (laser diode: 409 nm, 50 ps pulsewidth, 1 MHz repetition rate). The excitation density is 0.2 W cm^{-2}. (b) Short and long time constants, τ_1 and τ_2, deduced from biexp. fits in (a) together with the average lifetime τ. (c) Radiative and non-radiative lifetimes τ_{rad} and τ_{nr} calculated from eqn (7) + (8).

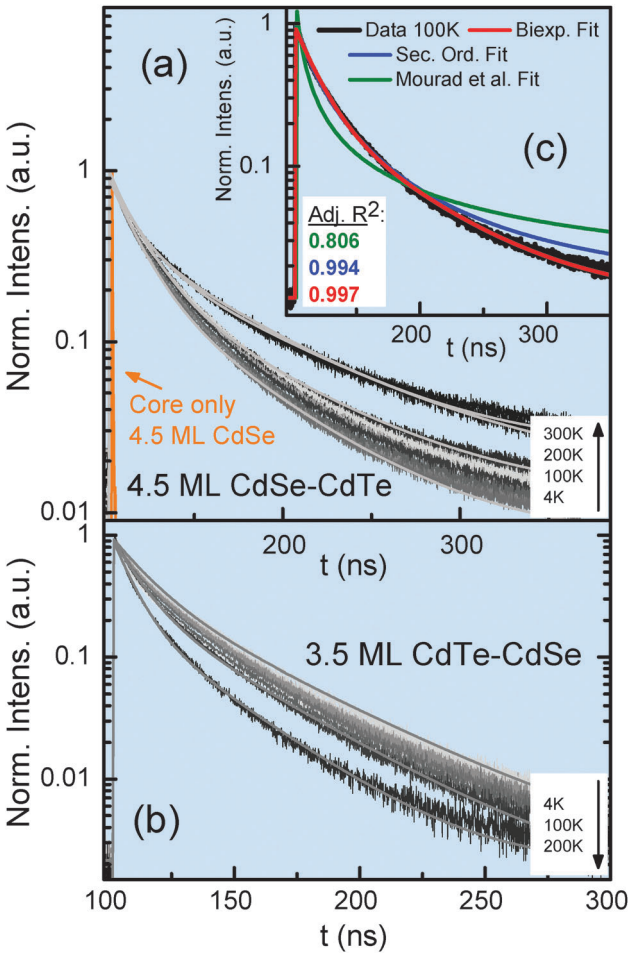

Fig. 4 Normalized time resolved photoluminescence of 4.5 ML CdSe–CdTe (a) and 3.5 ML CdTe–CdSe (b) nanoplatelets recorded at the spectral maximum of their respective type II emission bands shown in Fig. 1(b) and 2(b). Grey lines are biexponential fits for exemplary temperatures taking the convolution with the instrument response into account. Inset (c) shows a comparison of a biexponential fit, a second order decay fit and a fit according to Mourad *et al.*[27] for the 4.5 ML CdSe–CdTe platelets at an exemplary temperature of 100 K. An inspection of the fits and the fit quality determining adjusted R^2 values clearly shows that the biexp. model (red curve) is from the view of the χ^2 hypothesis test the most suitable and reproduces the data with a very high accuracy.

(a) and 3.5 ML CdTe–CdSe (b) type II hetero nanoplatelets show a strongly prolonged PL decay (Fig. 4). For comparison the 5.5 K decay curve of 4.5 ML core only platelets is shown in Fig. 4(a). The observed prolongation of the PL lifetime in the hetero platelets is due to the formation of a charge transfer state at the hetero interface, which can be an electron–hole pair (e–h pair) or an exciton state.[18] After a carrier pair is optically generated in CdSe or CdTe and has diffused fast to the hetero interface the electron wavefunction is mainly localized in CdSe, whereas the hole wavefunction is localized in the CdTe part of the junction.[23] This results in a spatially indirect state. The corresponding valence band (VB) and conduction band (CB) offsets at the junction have been determined to be 0.56 and 0.36 eV for CdSe–CdTe and CdTe–CdSe platelets.[23,25] However, it is still rather unclear whether the observed type II luminescence is related to an uncorrelated e–h pair or to a coulomb correlated exciton state.

This question can be answered by the PL decay dynamics of the excited species. In the case of excitons we again expect a biexponential PL decay as the hole mixing in the CdTe core will produce a bright and a dark exciton state as in the observations above for the core-only platelets.[26] In the case of a free e–h pair decay a Debye second order decay for the electron (n) and hole (p) densities according to $dn/dt = k_2(np)$ is expected. Under the valid assumption $n = p$ for optical excitation this results in a hyperbolic PL decay according to $\tilde{I}(t) = k_2 \times n_0^2/(1 + k_2 \times n_0 \times t)^2$ with initial concentration n_0 and decay rate k_2.[28] We tried to fit the transients (in Fig. 4(c)) with this function but obtained rather limited agreement and systematic deviations on long timescales with respect to the resulting χ^2 so that this model cannot reproduce the data. However, it has been pointed out that the polarization field generated by carrier separation at the junction may alter the decay kinetics and its rate constant k_2. Following Mourad *et al.*[27] the rate constant $k_2 = \gamma n$ is then proportional to the carrier density with a proportionality constant γ. This results in an altered PL decay function

$\tilde{I}(t) = \gamma \times {n_0}^2/(1 + \gamma \times n_0 \times t)^{3/2}$ which also does not fit our data appropriately (Fig. 4(c)). In contrast to these e–h pair recombination based models all PL decay results $\tilde{I}(t)$ in Fig. 4 can be well fitted by biexponentials

$$\tilde{I}(t) = A_1 \times e^{-t/\tau_1} + A_2 \times e^{-t/\tau_2} \quad (1)$$

as indicated by light grey lines in Fig. 4(a) and (b) for several temperatures. The inset of Fig. 4(c) displays a comparison of the three fit models for an exemplary temperature of 100 K, clearly indicating the superior agreement of the biexponential fit (red) with the measured data so that from the viewpoint of the χ^2 hypothesis test it is the most suitable model. Therefore it can be concluded that the predominant species causing the observed (red shifted) type II emission is related to exciton recombination and not e–h pairs.

Fig. 5(a) shows the resulting time constants τ_1 and τ_2 of the biexponential fits (Fig. 4(a)) for our temperature range from 4 to 300 K. The shorter time constant seems to be practically temperature independent, whereas the longer one exhibits a significant increase with temperature. Using these results we calculate the average lifetime of both components as[29]

$$\tau = \frac{\int_0^\infty t \cdot \tilde{I}(t)\mathrm{d}t}{\int_0^\infty \tilde{I}(t)\mathrm{d}t} = \frac{\sum_i A_i \tau_i^2}{\sum_i A_i \tau_i} \quad (2)$$

and plot it in Fig. 5(a). The observed PL lifetime $\tau(T)$ is related to the quantum yield $\eta(T)$, the intrinsic radiative lifetime τ_{rad} and the non-radiative lifetime τ_{nr} by

$$\tau(T) = \left(\frac{1}{\tau_{rad}(T)} + \frac{1}{\tau_{nr}(T)}\right)^{-1} = \tau_{rad}(T) \times \eta(T). \quad (3)$$

Knowing the temperature dependent quantum yield $\eta(T)$ makes it possible to derive the radiative and non-radiative lifetimes from the measured $\tau(T)$. The temperature dependent quantum yield can be obtained from a measurement of the temperature dependent time-integrated PL $I(T)$ as $\eta(300\ \mathrm{K})$ has been determined by a dye referencing method.

$$\eta(T) = \frac{I(T)}{I(300\ \mathrm{K})}\eta(300\ \mathrm{K}) \quad (4)$$

Fig. 6 shows the temperature dependence of the time integrated luminescence for the CdSe core only and the two hetero platelet samples. The temperature dependence can be well fitted with a thermally activated quenching model according to:[30]

$$I(T) = \frac{I(0\ \mathrm{K})}{1 + C \times e^{-E_A/k_B T}} \quad (5)$$

Using again $\eta(T) = \frac{I(T)}{I(0\ \mathrm{K})}\eta(0\ \mathrm{K})$ we obtain the temperature dependent quantum efficiency as

$$\eta(T) = \frac{\eta(0\ \mathrm{K})}{1 + C \times e^{-E_A/k_B T}} \quad (6)$$

with the activation energy E_A and constant C. Fig. 6 shows the results of the temperature dependent quantum yield and the fits to eqn (6) using $\eta(300\ \mathrm{K})$ determined by referencing to Rhodamine 6G. It can be seen that at low temperatures the quantum yield of our hetero platelets approaches about 70%. It drops to 19 and 13% for the CdSe–CdTe and CdTe–CdSe hetero platelets at room temperature, comparable to the core only platelets. The corresponding activation energies for the PL quenching deduced from the fits in Fig. 6 are 16 meV (4.5 ML core only), 50 meV (4.5 ML CdSe–CdTe) and 31 meV

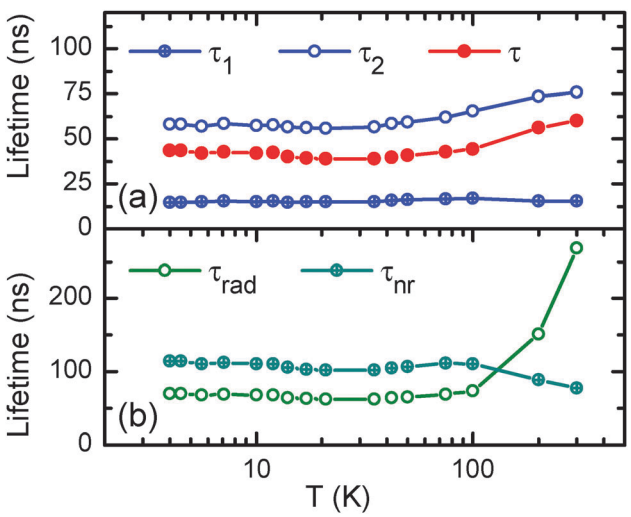

Fig. 5 CdSe–CdTe nanoplatelets of 4.5 ML: (a) time constants τ_1 and τ_2 from biexponential fits to Fig. 4(a) recorded at the spectral maximum of the type II emission band in Fig. 1(b) as well as the average lifetime τ derived from eqn (2). (b) Radiative and non-radiative lifetimes calculated from eqn (7) + (8).

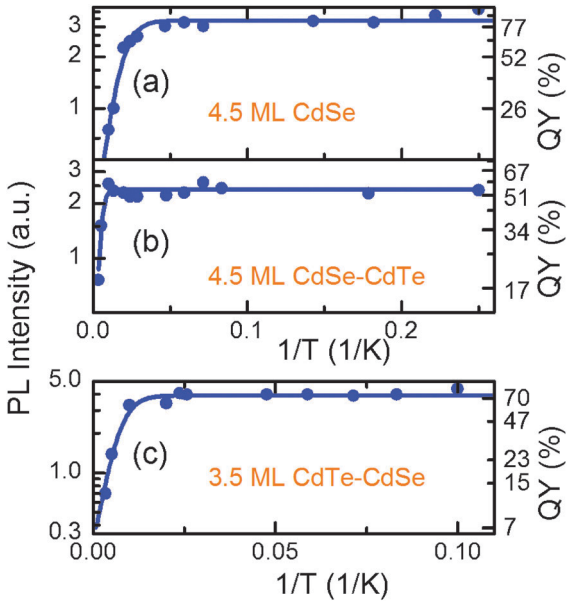

Fig. 6 Arrhenius plots of the spectrally and time-integrated photoluminescence of (a) 4.5 ML CdSe core only, (b) 4.5 ML CdSe–CdTe and (c) 3.5 ML CdTe–CdSe nanoplatelets and the temperature dependent quantum yield. Excitation conditions identical to Fig. 4.

(3.5 ML CdTe–CdSe). With the knowledge of $\eta(T)$ we can calculate the temperature dependence of the radiative

$$\tau_{rad}(T) = \frac{\tau(T)}{\eta(T)} \quad (7)$$

and non-radiative lifetime

$$\tau_{nr}(T) = \left(\frac{1}{\tau(T)} - \frac{1}{\tau_{rad}(T)}\right)^{-1} = \tau(T)(1-\eta(T))^{-1}. \quad (8)$$

The resulting temperature dependence of the radiative and non-radiative lifetime for the 4.5 ML core only and CdSe–CdTe hetero nanoplatelets is shown in Fig. 3(c) and 5(b). Two trends can be identified: while the non-radiative lifetime is decreasing with temperature the radiative lifetime increases with temperature. The increase of the radiative lifetime with temperature in a 2D system is related to the giant oscillator strength effect (GOST) in 2D.[5,31,32] A thermal redistribution of the generated excitons leads to a temperature increasing fraction of excitons that cannot decay radiatively since their **k**-vector is outside the radiative light cone. This phenomenon prolongs the overall decay of the photogenerated excitons with increasing temperature since the out of light cone scattering processes are thermally activated. The effect leads to an increase of the radiative lifetime with temperature from 70 to 270 ns for hetero nanoplatelets and from 0.3 to 1.8 ns for our core only nanoplatelets. According to Feldmann *et al.*[31] the radiative lifetime $\tau_{rad}(T)$ of a 2D exciton is related to its homogeneous transition linewidth $\Delta(T)$ by $\tau_{rad}(T) = F\Delta(T)/(1 - e^{-\Delta(T)/k_BT})$, with F a constant involving the exciton binding energy and the transition oscillator strength. Following Achtstein *et al.*[5] the homogeneous linewith of excitons in CdSe nanoplatelets can be modeled as $\Delta(T) = \Gamma_0 + \Gamma_A T + \Gamma_{LO}/(e^{E_{LO}/k_BT} - 1)$ with the zero temperature homogeneous linewidth Γ_0 and the coupling constants to acoustic (Γ_A) and LO-phonons (Γ_{LO}). Thereby the strong increase of the radiative lifetime with temperature in our core and core–lateral shell platelets can be understood as a suppression of the radiative recombination due to the increase of the homogeneous exciton linewidth with temperature. The above mentioned effect of a moderate increase of the radiative lifetime with temperature further indicates that excitons and not e–h pairs are present in the hetero platelets. In the case of free electron–hole pair recombination a far stronger temperature dependence of the bimolecular recombination coefficient k_2 according to $k_2 \propto (k_BT)^{-3/2}$ would be expected.[33] For example from 4 to 200 K a decrease of the radiative rate by a factor of $\sim$350 in k_2 would result in a prolongation of the radiative decay time τ_{rad} ($\propto 1/k_2$) by more than two orders in magnitude. This is clearly not reflected in the experimental results on the radiative lifetime and, in line with the findings above, rules out the presence and decay of electron–hole pairs.

In contrast to the mentioned radiative processes also non-radiative processes like exciton trapping and decay at defects take place. These non-radiative channels can be seen as temperature activated processes, as the mobile excitons have to overcome some activation energy to move to a defect or an exciton quenching site. Since they are thermally activated, the non-radiative rate increases with temperature and equivalently the non-radiative lifetime decreases as observed in Fig. 5(b). The thermally activated non-radiative processes are in line with the observed decrease of luminescence intensity with temperature (Fig. 6) since a larger fraction of excitons then decays non-radiatively.

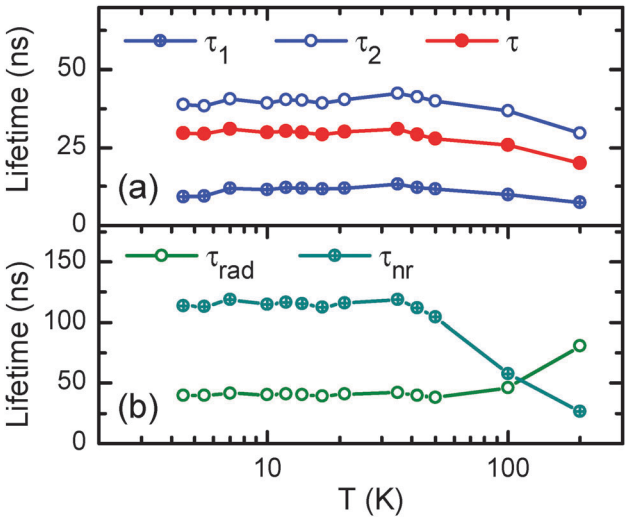

Fig. 7 (a) Time constants τ_1 and τ_2 from biexponential fits to Fig. 4 for 3.5 ML CdTe–CdSe nanoplatelets recorded at the spectral maximum of the type II emission band in Fig. 2. (b) Radiative and non-radiative lifetimes calculated from eqn (7) + (8).

In Fig. 7 we investigate analogously the temperature dependence of the radiative and non-radiative lifetime of our inverse 3.5 ML CdTe–CdSe nanoplates. Again from biexponential fits in Fig. 4(b) we derive the corresponding average lifetime in Fig. 7(a) and from that the temperature dependence of the radiative and non-radiative lifetimes in Fig. 7(b). While the non-radiative lifetime is with $\sim$120 ns comparable to the 4.5 ML CdSe–CdTe nanoplatelets at low temperatures, it decreases above 40 K more strongly leading to an overall decreasing average lifetime with temperature. This stronger impact of non-radiative processes in the inverse structure can be seen also in Fig. 6(c), where the intensity drop of the PL emission and quantum yield with temperature is stronger as compared to the 4.5 ML CdSe–CdTe platelet case. An explanation for this observed difference between the normal and inverse structure may be a synthesis related higher CdTe–CdSe interfacial defect density in the inverse type II structure or more defects at the edges of the outer CdSe lateral shell. Also if the electron trap density in the CdSe lateral shell is higher than the hole trap density in the CdTe lateral shell a difference in the non-radiative lifetimes for the CdSe–CdTe and CdTe–CdSe heterostructures may be the result. A stronger contribution of thermally activated nonradiative channels leads to a more strongly decreasing average lifetime with temperature for the 3.5 ML CdSe–CdTe plates (Fig. 7(a)), while the much weaker thermally activated nonradiative contribution in the 4.5 ML CdTe–CdSe platelets leads to the observation that the average lifetime is dominated by the prolongation of the radiative decay rate due to the giant oscillator strength effect (Fig. 5(a)).

However, even with the occurrence of relevant non-radiative recombination channels the CdSe–CdTe and inverse CdTe–CdSe

hetero platelets show much longer average (10–60 ns) and radiative (50–270 ns) lifetimes as compared to core only plates (with about 0.250 ns average and ~1 ns radiative lifetime) and CdSe–CdS type I nanoplates.[23] Therefore it is possible to engineer the decay dynamics in these 2D CdSe nanoparticles by the introduction of a lateral hetero transition. The experimental results clearly indicate that the ~100 fold lifetime prolongation is related to the formation of spatially indirect excitons being stable even at room temperature and not uncorrelated electron hole pairs. The long (carrier) lifetimes are desirable for photonic applications, however an application for photovoltaics is complicated since the spatially separated carriers cannot be extracted without biasing the hetero transition to ionize these spatially indirect excitons. Nevertheless the platelets may be very suitable as broad gain media in lasing applications due to their long exciton lifetime and possible low lasing threshold. The long radiative lifetimes let us also expect spectrally narrow single platelet emissions if the inhomogeneous ensemble broadening is overcome by single particle measurements.

3 Conclusions

We have investigated the temperature-dependent decay kinetics of type II CdSe–CdTe and CdTe–CdSe core–lateral shell nanoplatelets having quantum yields comparable to core-only platelets. A kinetic analysis of the photoluminescence (PL) decay and a measurement of the temperature dependent quantum yield are used to reveal for the first time the temperature dependence of the radiative and non-radiative lifetime of core only and hetero nanoplatelets. The observed increase of the radiative lifetime with temperature is in line with the predicted increase due to the giant oscillator strength effect in 2D and thus attributed to an increase of the homogeneous transition linewidth with temperature, while we can exclude bimolecular e–h pair recombination by decay kinetics and its temperature dependence. Our findings are indicative of the presence of charge carriers in the form of excitons in the nanoplatelets. In comparison to core only platelets we observe a significant prolongation of the radiative lifetime by two orders of magnitude in type II nanoplatelets, so that we expect that the radiative lifetime can be tuned by a heterojunction *via* confinement and band offsets. The analysis of the CdSe–CdTe and CdTe–CdSe hetero platelet PL decay shows that it is biexponential. This again indicates that predominantly spatially indirect excitons are present at the hetero junction and not ionized e–h pairs. These findings suggest that hetero nanoplates are less suitable for applications in solarcells, since generated carriers are coulomb correlated. On the other hand lasing applications might strongly benefit from a broad gain spectrum generated by the excitonic type II transition.

Acknowledgements

R. S., U. W. and A. W. A acknowledge funding by DFG projects WO477/32 and AC290/1. A. C. acknowledges financial support from the Basque Government within the Etortek IE11-304 program. M. A. acknowledges partial financial support from the Chemreagents program. A. P. acknowledges partial financial support from the Electronics and Photonics program.

References

1 M. A. El-Sayed, *Acc. Chem. Res.*, 2004, **37**, 326–333.
2 A. L. Efros and M. Rosen, *Ann. Rev. Mat. Sci.*, 2000, **30**, 475–521.
3 S. Ithurria and B. Dubertret, *J. Am. Chem. Soc.*, 2008, **130**, 16504–16505.
4 S. Ithurria, M. D. Tessier, B. Mahler, R. P. S. M. Lobo, B. Dubertret and A. L. Efros, *Nat. Mater.*, 2011, **10**, 936–941.
5 A. W. Achtstein, A. Schliwa, A. Prudnikau, M. Hardzei, M. V. Artemyev, C. Thomsen and U. Woggon, *Nano Lett.*, 2012, **12**, 3151–3157.
6 L. T. Kunneman, M. D. Tessier, H. Heuclin, B. Dubertret, Y. V. Aulin, F. C. Grozema, J. M. Schins and L. D. A. Siebbeles, *J. Phys. Chem. Lett.*, 2013, **4**, 3574–3578.
7 A. W. Achtstein, A. V. Prudnikau, M. V. Ermolenko, L. I. Gurinovich, S. V. Gaponenko, U. Woggon, A. V. Baranov, M. Y. Leonov, I. D. Rukhlenko, A. V. Fedorov and M. V. Artemyev, *ACS Nano*, 2014, **8**, 7678–7686.
8 C. She, I. Fedin, D. S. Dolzhnikov, A. Demortière, R. D. Schaller, M. Pelton and D. V. Talapin, *Nano Lett.*, 2014, **14**, 2772–2777.
9 R. Scott, A. W. Achtstein, A. Prudnikau, A. Antanovich, S. Christodoulou, I. Moreels, M. Artemyev and U. Woggon, *Nano Lett.*, 2015, **15**, 4985–4992.
10 A. W. Achtstein, A. Antanovich, A. Prudnikau, R. Scott, U. Woggon and M. Artemyev, *J. Phys. Chem. C*, 2015, **119**, 20156–20161.
11 S. J. Lim, W. Kim and S. K. Shin, *J. Am. Chem. Soc.*, 2012, **134**, 7576–7579.
12 Z. Li and X. Peng, *J. Am. Chem. Soc.*, 2011, **133**, 6578–6586.
13 K. Yu, B. Zaman, S. Romanova, D.-s. Wang and J. A. Ripmeester, *Small*, 2005, **1**, 332–338.
14 A. M. Smith and S. Nie, *Acc. Chem. Res.*, 2010, **43**, 190–200.
15 C. d. M. Donega, *Chem. Soc. Rev.*, 2011, **40**, 1512–1546.
16 D. Dorfs, T. Franzl, R. Osovsky, M. Brumer, E. Lifshitz, T. A. Klar and A. Eychmüller, *Small*, 2008, **4**, 1148–1152.
17 C. H. Wang, T. T. Chen, Y. F. Chen, M. L. Ho, C. W. Lai and P. T. Chou, *Nanotechnology*, 2008, **19**, 115702.
18 C.-H. Chuang, S. S. Lo, G. D. Scholes and C. Burda, *Phys. Chem. Lett.*, 2010, **1**, 2530–2535.
19 D. Oron, M. Kazes and U. Banin, *Phys. Rev. B: Condens. Matter Mater. Phys.*, 2007, **75**, 035330.
20 K. Gong, Y. Zeng and D. F. Kelley, *J. of Phys. Chem. C*, 2013, **117**, 20268–20279.
21 C. de Mello Donegá, *Phys. Rev. B: Condens. Matter Mater. Phys.*, 2010, **81**, 165303.
22 Y. Kobayashi, C.-H. Chuang, C. Burda and G. D. Scholes, *The Journal of Physical Chemistry C*, 2014, **118**, 16255–16263.
23 A. V. Antanovich, A. V. Prudnikau, D. Melnikau, Y. P. Rakovich, A. Chuvilin, U. Woggon, A. W. Achtstein and M. V. Artemyev, *Nanoscale*, 2015, **7**, 8084–8092.

24 Y. Kelestemur, M. Olutas, S. Delikanli, B. Guzelturk, M. Z. Akgul and H. V. Demir, *J. Phys. Chem. C*, 2015, **119**, 2177–2185.
25 S. Pedetti, S. Ithurria, H. Heuclin, G. Patriarche and B. Dubertret, *J. Am. Chem. Soc.*, 2014, **136**, 16430–16438.
26 L. Biadala, F. Liu, M. D. Tessier, D. R. Yakovlev, B. Dubertret and M. Bayer, *Nano Lett.*, 2014, **14**, 1134–1139.
27 D. Mourad, J.-P. Richters, L. Gérard, R. André, J. Bleuse and H. Mariette, *Phys. Rev. B: Condens. Matter Mater. Phys.*, 2012, **86**, 195308.
28 I. Pellant and J. Valenta, *Luminescence Spectroscopy of Semiconductors*, Oxford, 2012.
29 M. Jones, S. S. Lo and G. D. Scholes, *J. Phys. Chem. C*, 2009, **113**, 18632–18642.
30 D. Valerini, A. Creti, M. Lomascolo, L. Manna, R. Cingolani and M. Anni, *Phys. Rev. B: Condens. Matter Mater. Phys.*, 2005, **71**, 235409.
31 J. Feldmann, G. Peter, E. O. Göbel, P. Dawson, K. Moore, C. Foxon and R. J. Elliott, *Phys. Rev. Lett.*, 1987, **59**, 2337–2340.
32 A. Naeem, F. Masia, S. Christodoulou, I. Moreels, P. Borri and W. Langbein, *Phys. Rev. B: Condens. Matter Mater. Phys.*, 2015, **91**, 121302.
33 T. H. Gfroerer, L. P. Priestley, M. F. Fairley and M. W. Wanlass, *J. Appl. Phys.*, 2003, **94**, 1738–1743.